

Dynamic Calibration of a Multi-Component Force-/Torque Transducer

Jan Schleichert, Thomas Fröhlich

Institute for process measurement and sensor technology, Department of mechanical engineering
Ilmenau University of Technology, D-98684 Ilmenau, Germany, jan.schleichert@tu-ilmenau.de

Abstract

Multi-Component Force-/Torque Transducers are used in applications where the direction of the force- and torque vectors as well as their magnitude are unknown and time-dependent such as robotics, flow measurement or nondestructive testing. In contrast to the measurement task the calibration of those Sensors is only done statically in most cases. When the measurands are getting closer to the sensors resonance frequency, the usage of static calibration factors leads to deviations in the measurement. A dynamic calibration can be used to identify the frequency responses of the sensor and is the basis for designing an appropriate filter that compensates these deviations. In this paper the dynamic properties of a multi-component force-/torque transducer are investigated using a calibration system based on a voice-coil actuator which allows the application of force with different waveforms. The results of the measurements are compared with results of FEM calculations and results of a static calibration and a compensation filter is designed.

1 Introduction

Strain gauge based force transducers are often used in applications that require the measurement of static or quasi-static forces. These measurements can be done using results of static calibration. In dynamic measurements, deviations caused by the use of static calibration coefficients increases when approaching the resonance frequency of the sensor. This paper deals with the dynamic force calibration of a multi-component force-/torque sensor designed for the application in Lorentz force velocimetry [1]. For the dynamic calibration a system is used that allows the use of various test signals to determine the system parameters of the force transducer [2]. Measurement results for the calibration of three force components are shown. Based on the estimated parameters, an inverse filter [3] is designed to calculate the dynamic input force from the measured output voltages of the sensor.

2 Measurement Setup

To perform a dynamic measurement of the multi-component measurement system, forces with frequencies of up to 1000 Hz were applied using a voice-coil actuator. For a complete characterization of the force components of the sensor, at least three independent measurements are required, with the actuator being aligned with each one of the three measurement axes. The force sensor is mounted in a fixed position while the voice-coil actuator is mounted in three different orientations on the force feed-in as can be seen from Figure 1. During every measurement the responses of all measurement axes are captured which allows the determination of the main responses and the crosstalk to other components.

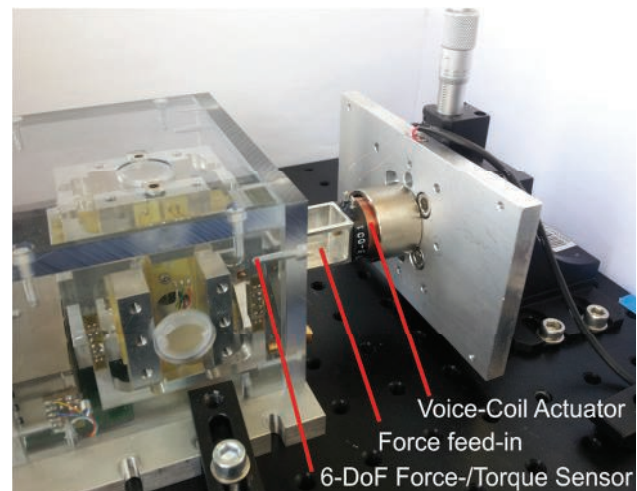


Figure 1: Force calibration of z-axis with voice-coil actuator

The actuator generates a Lorentz force proportional to the current, applied by a U/I-converter which translates the test signals created by a dSPACE digital signal processing unit [4]. The current through the coil is measured to calculate the acting force from the calibration constant of the actuator. The U/I converter has a constant transfer behavior of 101 mA/V up to a frequency of 10 kHz. Additional to creating the test signals and measuring the coil current, the dSPACE unit is used for simultaneous sampling of the output signals of the six channels of the force sensor. The dSPACE unit is controlled by a computer, which is responsible for processing the measured data and receiving the measuring parameters, such as the measuring time and type of test signal from the user.

3 System Identification

3.1 Signal Processing

To determine the transfer function the Fourier Transform is applied to the system's input signal $u(t)$ and output signal $y(t)$ giving

$$\mathcal{F}\{u(t)\} = U(j\omega); \quad \mathcal{F}\{y(t)\} = Y(j\omega)$$

Under the assumption that the system is linear, its frequency response can be determined as [5]:

$$G(j\omega) = \frac{Y(j\omega)}{U(j\omega)}$$

By the FFT, we obtain a discrete estimate for the system's frequency response:

$$\hat{G}(j\omega_i) = \frac{\hat{Y}(j\omega_i)}{\hat{U}(j\omega_i)}$$

where $\hat{Y}(j\omega_i)$ and $\hat{U}(j\omega_i)$ are respectively the FFT of the systems input and output signal and $i \in \{x \in \mathbb{N}^*: x \leq k\}$, with $k \in \mathbb{N}^*$ equal to the domain size of the discrete frequency response function. The systems gain $K(\omega_i)$ and phase shift $\varphi(\omega_i)$ are calculated through the following expressions:

$$K(\omega_i) = |\hat{G}(j\omega_i)|; \quad \varphi(\omega_i) = \arg(\hat{G}(j\omega_i))$$

The input signal $u(t)$ should contain every frequency component that is relevant for the analysis. Here we use the Maximum length binary sequence (MLBS) and the Chirp-Signal.

The chirp signal (Figure 2) consists of a sine function with time-dependent frequency. This signal is given by the following function:

$$u(t) = \sin\left(2\pi\left(\frac{f_1 - f_0}{2f_1}t^2 + f_0t\right)\right)$$

where f_0 and f_1 are the initial and final frequency. On mechanical systems with resonance, the chirp signal must be carefully applied in order to avoid excessive excitation of the system at its resonance frequency.

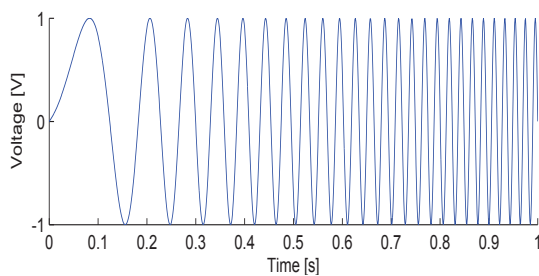


Figure 2: Chirp signal

The MLBS signal (Figure 3, [6]) is a pseudo random, time-discrete, binary signal. Like the pseudo-random white noise, this signal is capable to excite different frequency components simultaneously.

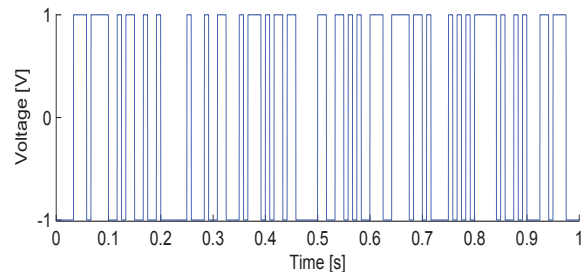


Figure 3: Maximum length binary sequence (MLBS)

3.2 Frequency response of the amplifier

As the output signals of the transducer are in the range of some mV, the frequency response of the sensor cannot be measured accurately without amplification. Therefore a six-channel analog preamplifier based on Linear Technology LT1167 instrumentation amplifiers and a constant voltage bridge supply is set up and needs to be identified separately from the force sensor to determine its influence on the measured response. This measurement is done by using a dummy Wheatstone bridge circuit with the Chirp-signal described above as excitation-signal for the bridge.

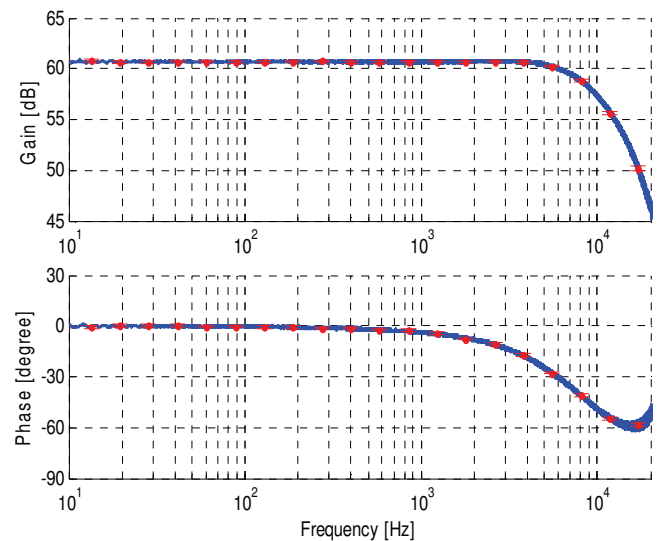


Figure 4: Frequency response of the amplifier (blue) with standard deviation over 20 measurements (red)

The amplifier was set to gain of 61 dB and reaches a corner frequency of 9 kHz, which corresponds approximately to the datasheet value of 12 kHz given for a gain of 1000. The frequency-dependent change of gain and phase of the amplifier is negligible in the frequency range where the sensor is identified. Therefore the amplifier can be considered by a constant factor in the measured transfer function of the sensor.

3.3 Parametric Identification

All axes of the sensor were measured using the chirp signal. For system identification, the mean values of 20 measurements were used. These results are very similar to the frequency response of the second order transfer function

$$G(s) = \frac{K\omega_0^2}{s^2 + 2\xi\omega_0s + \omega_0^2},$$

with $K, \omega_0 \in \mathbb{R}^+$ and $\xi \in \{x \in \mathbb{R} : 0 < x < 1\}$. Through the parametric optimization of the error function

$$e(K, \omega_0, \xi) = \int_{\omega_1}^{\omega_2} (|G(j\omega)| - G_M(\omega))^2 d\omega,$$

the transfer function $G(s)$ can be fitted to the measured frequency response data $G_M(\omega)$, and the parameters K , ω_0 and ξ can be determined. This was done for all axes of the multicomponent sensor with $\omega_1 = 10$ Hz and $\omega_2 = 200$ Hz. The result of the identification process is shown for the z-axis in Figure 5.

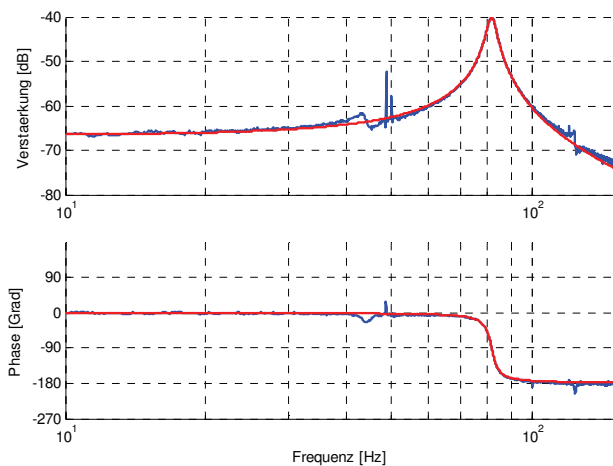


Figure 5: Measured Frequency response of the sensors z-axis (blue) and frequency response of identified model (red)

Characteristics of the measured signal like disturbances at about 50 Hz, caused by the alternating-current electric power supply or coupling between the axes at resonance frequencies (at approx. 45, 120 Hz) are not considered by the transfer function $G(s)$. For every axis a transfer function model was fitted. The identified parameters including their uncertainties obtained from the fitting procedure are shown in Table 1.

Table 1: Results of the parametric identification

Axis	X	Y	Z
K	4.0905e-04	2.9794e-04	4.6903e-04
$u(K)$	7.4766e-07	1.6344e-06	7.0869e-07
ω_0 (Hz)	84.9673	64.6189	81.8081
$u(\omega_0)$ (Hz)	0.8447	0.8181	0.7782
ξ	0.0266	0.0271	0.0238
$u(\xi)$	6.9215e-05	1.6664e-04	5.7882e-05

4 Simulation

To calculate the frequency response of the sensor, a harmonic analysis in ANSYS Workbench was done. The simulation provides information about the mode shapes of the oscillation as shown in Figure 6.

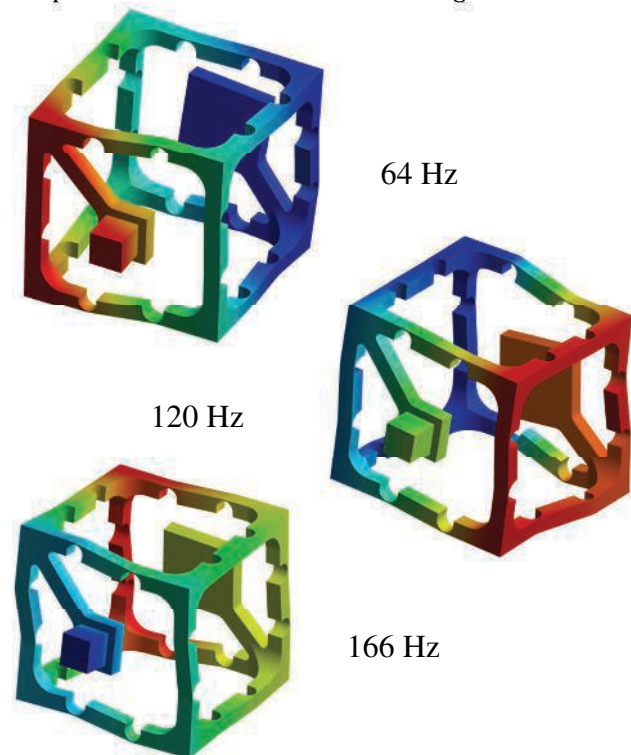


Figure 6: Mode shapes of the sensor when excited by a force in y-direction

The local strain at the application areas of the strain gauges can be calculated as well. The frequency response was determined firstly for every single strain gauge. Four strain gauge responses were combined to obtain the output response of a measurement bridge. The bridge signals were used to calculate the output signal of the sensor which is shown in Figure 7.

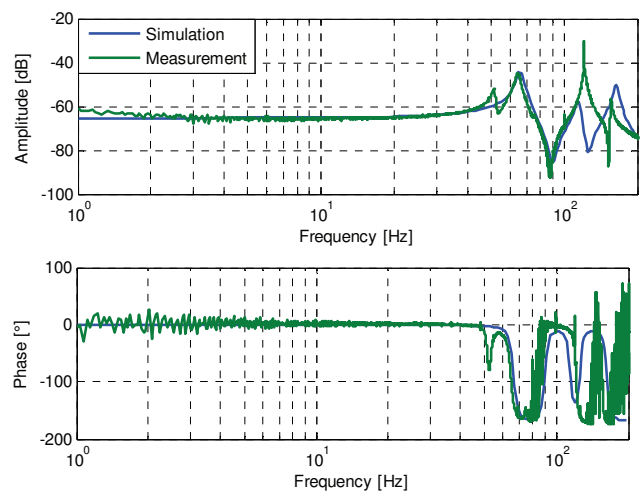


Figure 7: Comparison of simulation results and measurement for frequency response of y-axis.

The simulation shows a good agreement with the measurement to a frequency of about 100 Hz. Due to the inaccuracy of modeling of the mass and mass distribution of the voice-coil and the lever, the resonance frequency and the disturbances deviate from the measurement result.

5 Filter Design

As shown above, the sensor has a frequency dependent sensitivity which leads to measurement errors if a static calibration is applied to dynamic measurements. Based on the model of the measurement axes, a filter can be designed to obtain the correct input signal by deconvolution of the output signal with the inverse model of the measurement system [7]. Until their first resonance frequency the measuring axes don't have many disturbances or crosstalk and can be modeled by a second order transfer function. To determine the discrete filter from the identified transfer functions they are discretized using the bilinear transformation

$$s = \frac{2}{T} \frac{z-1}{z+1}$$

The discrete transfer function is given by

$$G_d(z) = G_c(s) \Big|_{s=\frac{2}{T} \frac{z-1}{z+1}}$$

A digital filter can be expressed in the following form

$$H(z) = \frac{B(z)}{A(z)} = \frac{b_0 + b_1z^{-1} + b_2z^{-2} + \dots + b_Nz^{-N}}{1 + a_1z^{-1} + a_2z^{-2} + \dots + a_Mz^{-M}}$$

By comparison of the coefficients of the discrete transfer function $G_d(z)$ with $H(z)$ the filter coefficients can be determined. The inverse filter coefficients are given by $H^{-1}(z)$. To get a stable FIR-filter the denominator is set to a constant value given by the sum of all denominator coefficients. Through the filtering a flat frequency response is achieved and signals at high frequencies are strongly amplified. To reduce noise on the filter output and reduce the influence of higher resonances, another lowpass filter is needed to attenuate the signal at frequencies above the desired measurement bandwidth.

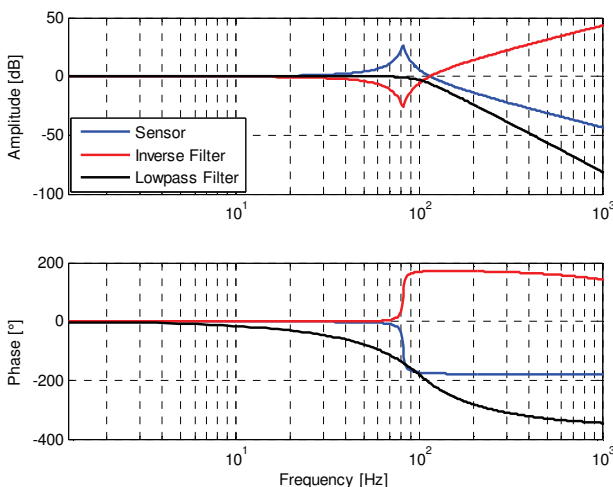


Figure 8: Sensor and filter responses for z-axis. The amplitude responses are normalized to a gain of 0 dB.

Figure 9 shows the sensor response to an input signal, the response of the inverse filter with and without the additional lowpass filter together in time-domain.

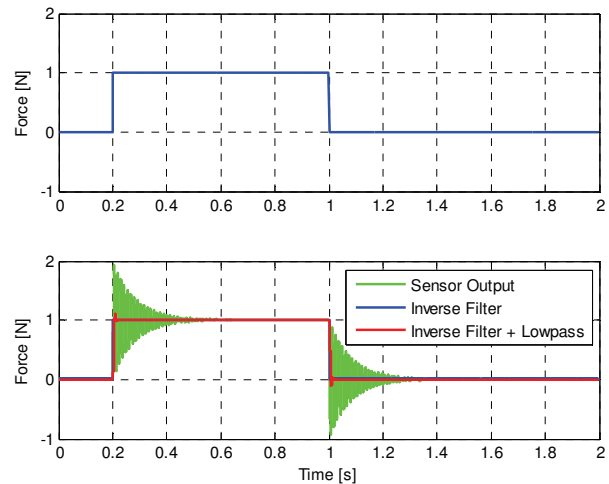


Figure 9: Input signal (top) and corresponding sensor output (bottom) with static (green) and dynamic calibration (blue, red)

6 Conclusion

In this paper, the force measuring axes of a multi-component force-/torque sensor is calibrated dynamically by using a voice-coil actuator. From the frequency responses the parameters of a second-order transfer function model for every axis are identified. Then the results of a FEM-simulation are compared to measurement results. An inverse filter is designed in order to decrease the measurement error at operating frequencies close to resonance.

7 Literature

- [1] Heinicke, C. et al.: Interaction of a small permanent magnet with a liquid metal duct flow, *J. Appl. Phys.* 112, 124914, 2012
- [2] Schleichert, J. et al.: Dynamic characterization of a multi-component force transducer using a Lorentz force load changer. *Technische Universität Ilmenau; IWK 58: 2014.09.08-12.*
- [3] Eichstädt, S.; Link, A.; Elster, C.: Dynamic Uncertainty for Compensated Second-Order Systems. *Sensors* 2010, 10, 7621-7631.
- [4] https://www.dspace.com/de/gmb/home/products/hw/modular_hardware_introduction.cfm (19.02.2015)
- [5] Lunze, J., *Regelungstechnik 1: Systemtheoretische Grundlagen, Analyse und Entwurf Einschleifiger Regelungen*, Springer 2013, 9th edition, 724 pages
- [6] Isermann, R., *Identifikation dynamischer Systeme 1: Grundlegende Methoden*, Springer 1992, 2nd edition, 352 pages
- [7] S Eichstädt et al: Deconvolution filters for the analysis of dynamic measurement processes: a al, 2010 *Metrologia* 47 522